

Spatial and temporal variability of methane emissions and environmental conditions in a hyper-eutrophic fishpond

Petr Znachor^{1,2}, Jiří Nedoma¹, Vojtech Kolar^{1,2}, Anna Matoušů¹

¹Biology Centre of Czech Academy of Sciences, v.v.i., Institute of Hydrobiology, Na Sádkách 7, České Budějovice, 37005, Czech Republic

²Faculty of Science, University of South Bohemia, Branišovská 1760, České Budějovice, 37005, Czech Republic

Correspondence to: Anna Matoušů (anna.matousu@gmail.com)

Abstract. Estimations of methane (CH₄) emissions are often based on point measurements using either flux chambers or a transfer coefficient method which may lead to strong underestimation of the total CH₄ fluxes. In order to demonstrate more precise measurements of the CH₄ fluxes from an aquaculture pond, using higher resolution sampling approach we examined the spatiotemporal variability of CH₄ concentration in the water, related fluxes (diffusive and ebullitive) and relevant environmental conditions (temperature, oxygen, chlorophyll-a) during three diurnal campaigns in a hyper-eutrophic fishpond. Our data show remarkable variance spanning several orders of magnitude while diffusive fluxes accounted for only a minor fraction of total CH₄ fluxes (4.1–18.5 %). Linear mixed-effects models identified water depth as the only significant predictor of CH₄ fluxes. Our findings necessitate complex sampling strategies involving temporal and spatial variability for reliable estimates of the role of fishponds in a global methane budget.

Keywords: aquaculture, emissions, fishpond, freshwater, heterogeneity, methane

23 **1 Introduction**

24 Freshwater aquaculture ponds (fishponds) represent man-made counterparts to natural shallow lakes (Scheffer,
25 2004) which are mainly used for fish production (mostly of common carp, *Cyprinus carpio* L.) and water retention
26 in the landscape. Fishponds serve also as secondary biotope for various organisms (Kolar et al., 2021), supporting
27 noteworthy animal and plant diversity (Pokorný and Hauser, 2002). However, most fishponds suffer from high
28 fish stock densities, excessive carbon and nutrient loading from supplemental fish feeding, sewage pollution, and
29 fertiliser runoffs from agricultural catchments or nutrient mobilisation from the anoxic sediment layers (Pechar,
30 2000). As a result, the trophic structure of plankton communities has shifted towards a reduction of large
31 zooplankton and massive development of phytoplankton, especially cyanobacterial blooms (Potužák et al., 2007),
32 limiting light penetration in the water column. Rapid changes in the intensity of biological processes such as
33 photosynthesis and respiration often result in pronounced daily or seasonal fluctuations in dissolved oxygen (Baxa
34 et al., 2021), signalling decreasing ecosystem stability. The extent of anoxia, accumulation of organic biomass,
35 and rapid heating of the shallow water during summer result in enhanced production of greenhouse gases (Grasset
36 et al., 2018, Zhang et al., 2021; Bartosiewicz et al., 2021).

37 Most concerning are CH₄ emissions as freshwater aquaculture systems release more than 6 Tg CH₄ yr⁻¹ (Yuan et
38 al., 2019). Methane can be emitted via several pathways: simple molecular diffusion, ebullition (in the form of
39 bubbles released from oversaturated sediments), plant-mediated flux (Bastviken et al., 2004), but also through so
40 far neglected pathways including aeration, emissions from dry/drying sediments, or dredged organic material
41 (Kosten et al., 2020). Among all, ebullition is considered the dominant pathway (van Bergen et al., 2019; Kosten
42 et al., 2020), which can contribute 50-96 % (Casper et al., 2000; Xiao et al., 2017; van Bergen et al., 2019; Yang
43 et al., 2020; Zhao et al., 2021) to the total CH₄ flux. Along with the second important pathway – molecular
44 diffusion, both exhibit high spatiotemporal variability due to various physical and biological factors acting on very
45 short time scales, for instance, temperature (van Bergen et al., 2019), nutrient loading (Zhang et al., 2021), CH₄
46 production rates (Zhou et al., 2019), CH₄ oxidation rates (Sanseverino et al., 2012), dissolved oxygen concentration
47 (Xiao et al., 2017), management regime (Yang et al., 2019), or the quality of organic matter in the sediment
48 (Schmiedeskamp et al., 2021). Recently, the direct involvement of phytoplankton in CH₄ production and emissions
49 has been emphasised (Yan et al., 2019; Bižić et al., 2020; Bartosiewicz et al., 2021). The complex interactions
50 between physical and biological factors lead to a dynamic and ever-changing environment, characterised by high
51 spatial and temporal variability of methane fluxes in ponds.

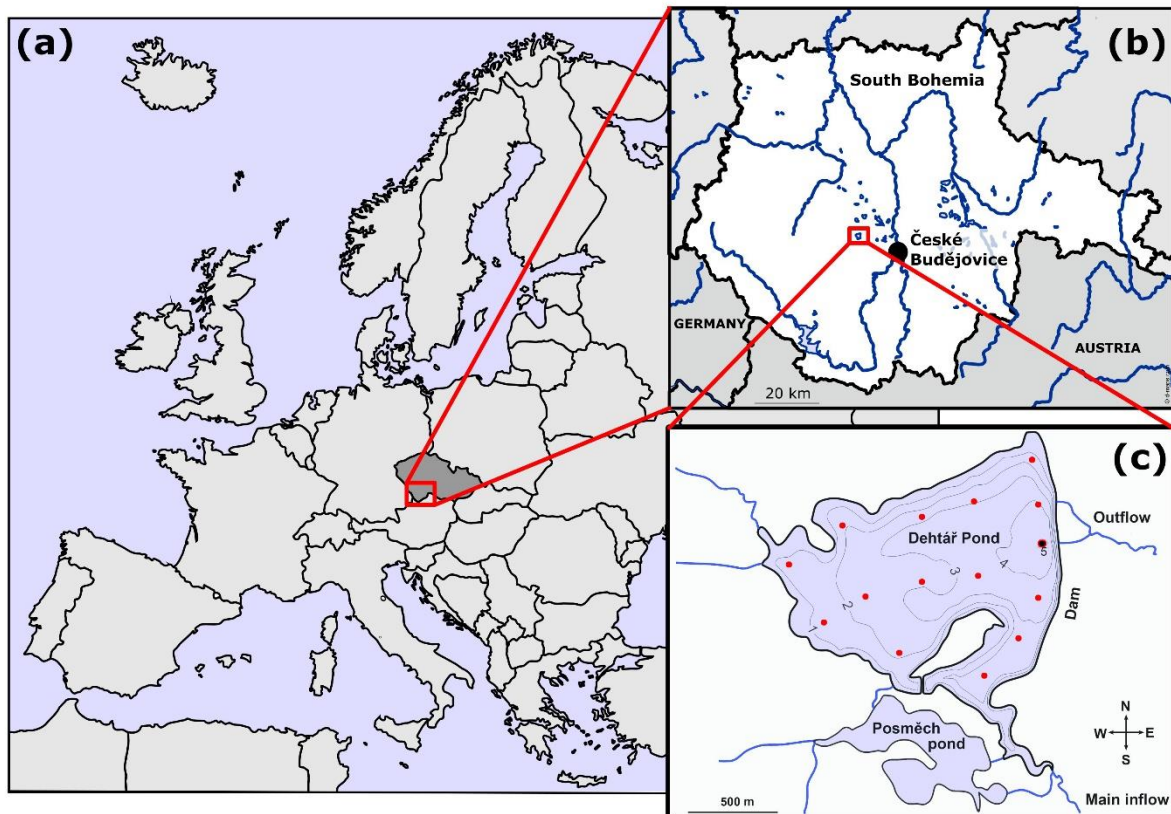
52 Although fishponds are recognised as powerful model systems for studies in ecology and evolutionary or
53 conservation biology (De Meester et al., 2005; Céréghino et al., 2008), the extent of environmental heterogeneity
54 in fishponds and shallow inland small waterbodies remains poorly understood (Ortiz and Wilkinson, 2021), largely
55 because the driving factors are either system-specific or highly variable on short time scales (Laas et al., 2012).
56 Most of current information on lentic ecosystem structure and function comes from single-site sampling, in which
57 measurements are taken over time at the deepest point in the lake, which does not sufficiently account for within-
58 lake spatial variation (Stanley et al., 2019). The motivation for our study was the growing concern about the role
59 of fishponds as important sources of CH₄ fluxes to the atmosphere (Wik et al., 2016). Unfortunately, the majority
60 of global CH₄ flux estimates rely on upscaling methods (DelSontro et al., 2018a) based on a limited number of
61 measurements that do not account for diurnal and seasonal variability or ecosystem spatial heterogeneity. Yang et
62 al. (2019) indicates that a larger number of spatial replicates over a number of months is mandatory to improve
63 the accuracy of whole-pond CH₄ flux estimates. The published research from other aquaculture studies have been
64 performed mainly in tropical and subtropical zones in fish or crab aquacultures (e.g., Hu et al., 2016; Ma et al.,
65 2018; Yang et al., 2019, 2020; Yuan et al., 2019, 2021). To better understand the spatial dynamics of CH₄ fluxes
66 and environmental heterogeneity in temperate freshwater shallow lake, we conducted a spatial sampling of the
67 hyper-eutrophic Dehtář fishpond (Czech Republic, Europe). Since the seasonal CH₄ production is strongly affected
68 by temperature, we focused on warm summer months where the total CH₄ fluxes were expected to be the highest
69 (Jansen et al., 2019). The objectives of our study were (i) to determine the spatial heterogeneity of CH₄ diffusive
70 and total fluxes and fundamental limnological variables (oxygen, temperature, chlorophyll-a) and their change
71 daily and monthly in the hyper-eutrophic pond, and (ii) to identify the factors that influence CH₄ fluxes to improve
72 our understanding of the importance of spatiotemporal variability for global estimates of CH₄ efflux to the
73 atmosphere.

74 **2 Material and Methods**

75 **2.1 Study site description**

76 The Dehtář fishpond (49° N, 14° E) is a shallow man-made lake (average and maximum depth: 2.4 and 6 m)
77 constructed in 1479 and used for polycultural, semi-intensive production of common carp (Potužák et al., 2016).
78 It lies in a flat agricultural landscape at 406.4 m above sea level in the upper Vltava River basin in South Bohemia
79 (Czech Republic) which is characteristic with its network of fishponds (Fig. 1b). Due to the orography of the

80 landscape, the Dehtář fishpond, surrounded by narrow belts of littoral vegetation and adjacent to grassland and
81 arable land, is exposed to wind, mainly from the northwest (for aerial photograph, see Suppl. Fig 1). The catchment
82 area is 91.4 km². The main inflow is the Dehtářský stream in the south, while several smaller tributaries flow in
83 from the west (Fig. 1c). The fishpond has a dam 234 m long and 10 m high, with two outlets and a safety spillway.
84 Covering 2.28 km², the Dehtář fishpond is among the ten largest fishponds in the Czech Republic, holding a
85 volume of 4.71×10^3 m³ and having a water residence time of 146-445 days (Potužák et al., 2016).



86

87 **Figure 1.** Location (a, b; copyright www.d-maps.com; https://d-maps.com/carte.php?num_car=2232&lang=en and https://d-maps.com/carte.php?num_car=265046&lang=en; modified) and bathymetric map (c; credit Jiří Jarošík) of the sampled Dehtář
88 fishpond: Blue lines indicate hydrological connections; red dots representing the sampling points. Highlighted sampling point
89 at the dam depicts the deepest site where vertical profiles were measured. Numbers indicate isobath depth.
90

91

92 2.2 Sampling design and measurement

93 To measure spatial heterogeneity and temporal changes in limnological parameters and methane fluxes, we
94 conducted three 36-hour surveys in summer 2019 (July 2-3, August 13-14, September 19-20). In the morning
95 (between 5-6 a.m.), we first measured surface values and vertical profiles of temperature, oxygen, and chlorophyll-
96 *a* concentration at the deepest point (see below for details). We subsequently installed 15 floating polyethylene
97 chambers (as shown in Fig. 1c), serving as fixed sampling sites and at the same time for accumulation of CH₄
98 fluxes (see further), starting in the western part of the fishpond. During installation (and further during each

99 sampling), temperature, pH, and oxygen concentration were measured at 0.3 m depth using the WTW 330i pH
100 meter and Oximeter (WTW, Weilheim, Germany). Vertical chlorophyll-*a* profiles were measured at each sampling
101 site using a submersible fluorescence probe (FluoroProbe, bbe Moldaenke, Kiel, Germany). From each site, the
102 average chlorophyll-*a* concentration in the surface layer (0-1 m depth) was used to assess the phytoplankton spatial
103 heterogeneity.

104 To minimise the chance that the differences observed among sites were due to time of day, we conducted repeated
105 measurements at the deepest point at the end of each sampling. This was relevant mainly to the initial measurement,
106 when the installation of all floating chambers took a total of 3 hours and 50 minutes. All other measurements, i.e.
107 the interval between the first and last sampling point, required approximately two hours each. If there was a change,
108 all values were corrected for the sampling time by linear interpolation:

$$109 \quad P_{corr} = P_t + (P_{end} - P_0) \times \frac{(t-t_0)}{(t_{end}-t_0)} \quad (1)$$

110 where P_{corr} is the corrected value of a parameter, P_t is its value measured at the time t , P_0 and P_{end} are parameter
111 values measured at the deepest point at the start (time t_0) and at the end (t_{end}) of the sampling. In the evening and
112 morning of the second day (roughly at 12 h intervals), we performed additional measurements of spatial
113 heterogeneity, allowing us to assess diurnal and nocturnal changes. In addition, samples for measuring CH_4
114 concentration in the surface water were collected at each site and analysed as described below. To assess diurnal
115 variations in thermal structure and oxygen concentration in the water column, we made vertical profile
116 measurements at the deepest point (Fig. 1c) at 3-6 h intervals using the YSI EXO 2 multiparametric probe (YSI
117 Inc., Yellow Springs, USA).

118 **2.3 Methane measurements**

119 Water samples for determining CH_4 concentration in the surface water were collected at all 15 sampling sites in
120 triplicates into 20 ml glass bottles. The bottles were capped bubble-free under water with black butyl rubber
121 stoppers (Ochs, Germany) and sealed with aluminium crimps. Immediately after sampling, the water samples were
122 preserved by injecting 100 μ l of concentrated sulfuric acid to stop the microbial activity (Bussmann et al., 2015).
123 The samples were processed within one week in the laboratory using a headspace technique according to
124 McAuliffe (1971). Methane concentration in the headspace was measured using an HP 5890 Series II gas
125 chromatograph (Agilent Technologies, USA) and calculated with the solubility coefficient given by Yamamoto et
126 al. (1976).

127 Methane diffusive fluxes (F) were then calculated for each sampling site indirectly using the 2-layer model with
128 the equation:

129 $F = k(C_{sur} - C_{eq})$ (2)

130 where C_{sur} is the CH_4 concentration in surface water in $\mu\text{mol L}^{-1}$, C_{eq} is the CH_4 concentration in surface water in
 131 equilibrium with the atmosphere in $\mu\text{mol L}^{-1}$, and k is the CH_4 exchange constant (cm h^{-1}). The atmospheric partial
 132 pressure of CH_4 was set to 1.8 ppm. To compute k values we first derived k_{600} estimates using a wind speed-based
 133 relationship according to Crusius and Wanninkhof (2003):

134 $k_{600} = 1.68 + (0.228 \times U_{10}^{2.3})$ (3)

135 where U_{10} represents the wind speed at 10 m height (in m.s^{-1} ; obtained from the nearby gauging station)
 136 approximated by $U_{10} = 1.22U$, where U is the wind speed at 1.5 m height. We then converted k_{600} to k using the
 137 eq. 4 according to Crusius and Wanninkhof (2003):

138 $k = k_{600} \left(\frac{Sc}{600}\right)^n$ (4)

139 where k_{600} is the gas transfer velocity for a Schmidt number (Sc) of 600; n is a wind speed-dependent conversion
 140 factor, for which we used $-2/3$ for $U_{10} < 3.7 \text{ m s}^{-1}$ (Jähne et al., 1987). The Schmidt number for CH_4 was calculated
 141 according to Wanninkhof (2014):

142 $Sc = 1909.4 - 120.78t + 4.1555t^2 - 0.080578t^3 + 0.000658t^4$ (5)

143 where t ($^{\circ}\text{C}$) is the water temperature at the time of CH_4 extraction. The parameter C_{eq} in Eq. (1) was determined
 144 from the equation:

145 $C_{eq} = \beta \times pCH_4$ (6)

146 where β is the solubility coefficient of CH_4 as a function of temperature according to Wiesenburg and Guinasso
 147 (1979), and pCH_4 is the partial pressure of CH_4 in the atmosphere.

148 To estimate total CH_4 fluxes from the water column to the atmosphere (i.e., diffusive and ebullitive fluxes), we
 149 measured CH_4 accumulation in open-bottom floating polyethylene chambers (volume 3.1 L; area 0.024 m^2). Each
 150 gas chamber was anchored at individual 15 fixed sampling sites, but allowed to float freely on the water surface.
 151 Gas was accumulating for approximately 12 h (each incubation had a start and end point) during particular
 152 sampling period, i.e., during the day and night periods. Afterwards, 30 ml of gas was carefully taken from each
 153 chamber, after mixing the headspace in the chamber, and stored in evacuated Exetainers[®] (Labco Limited, UK).
 154 Chambers were ventilated after each sampling period to reset the incubation conditions. Methane fluxes were
 155 calculated as the difference between initial background and final concentration in the chamber headspace and
 156 expressed on the 1 m^2 area of the surface level per day according to Bastviken et al. (2004).

157 **2.4 Background limnological parameters**

158 During each campaign, water samples for analysis of nutrient concentration and phytoplankton composition were
159 collected from the surface at the deepest point using a Friedinger sampler. Water transparency was measured using
160 a Secchi disk. Total phosphorus (TP) and soluble reactive phosphorus (SRP) were analysed spectrophotometrically
161 according to Kopáček and Hejzlar (1993) and Murphy and Riley (1962), respectively. Concentrations of NH_4^+ and
162 NO_3^- were determined according to the procedure of Kopáček and Procházková (1993) and Procházková (1959),
163 respectively. Phytoplankton samples were preserved with Lugol's solution and examined for species composition
164 with an inverted microscope (Olympus IMT-2). Weather data were obtained from the gauging station at the
165 fishpond dam.

166 2.5 Statistical analyses

167 Two-tailed paired Student's t-tests and Two-way ANOVA with post-hoc Tukey's multiple comparison test (Prism
168 9.3, GraphPad Software Inc., La Jolla, USA) tested for differences between diffusive and total CH_4 fluxes between
169 day and night and among three sampling campaigns, respectively. The percentage of data variability explained by
170 different factors (daytime, month and site) was calculated with the Two-way RM ANOVA. Contour graphs
171 illustrating changes in spatial heterogeneity of measured parameters were constructed in Surfer 10 (Golden
172 Software, Inc., Colorado, USA) using the kriging contouring method. Spatial heterogeneity was quantified for
173 each sampling by calculating the spatial variance (i.e., coefficient of variation of values measured at 15 sampling
174 sites; see, e.g. Fig 2):

$$175 \quad CV\% = 100 \times \frac{SD}{mean} \quad (7)$$

176 Higher spatial variance indicates increasing ecosystem patchiness. Linear mixed-effects models were used to
177 analyse the effects of O_2 , pH, temperature, and water depth on the CH_4 diffusive fluxes with the random effect of
178 time of day nested within the effect of sampling date. The most parsimonious model was obtained by a manual
179 backward selection, where we sequentially removed all insignificant predictors ($p > 0.05$) using likelihood ratio
180 tests implemented in the drop1 function (Zuur et al., 2009). We also compared the slopes of the month-specific
181 regression lines produced by the model using analysis of covariance (Zar, 1984). Linear mixed-effects models
182 were implemented in the lme4 package version 1.1-21 (Bates et al., 2015), and Kenward-Roger F-tests were
183 computed using the ANOVA Type II function from the pbkrtest package version 0.4-7 (Halekoh and Hojsgaard,
184 2014). The prediction of the resulting final model was visualised in the package ggeffects version 0.14.1 (Lüdtke,
185 2018). Package performance version 0.4.4 (Lüdtke et al., 2020) was used to calculate Nakagawa's R^2 of the linear
186 model. The statistical analyses were performed using R software (v. 3.5.2, R Core Team, 2018).

187 **3 Results**

188 **3.1 Weather and background fishpond characteristics**

189 Weather parameters varied among sampling campaigns. In July, clear skies prevailed with the daily air temperature
 190 above 30 °C (Table 1). During the August and September measurements, it was very cloudy, and daily air
 191 temperatures decreased to 22 and 18 °C, respectively. The water level was stable during the whole studied period
 192 with a monthly fluctuation of ~ 10 cm. Water transparency was low (15-40 cm), with an increasing trend towards
 193 the end of summer (Table 1). Concentrations of total phosphorus and soluble reactive phosphorus were high (Table
 194 1), consistent with a hyper-eutrophic state of the fishpond. In contrast, nitrogen concentrations were rather low,
 195 with ammonium nitrogen being the predominant form of inorganic N in the water (Table 1).

196 **Table 1:** Basic characteristics of the Dehtár fishpond during the studied period, measured at the surface at the deepest point.

	July	August	September
Weather	Clear sky, windy	Partly cloudy, no wind	Partly cloudy, no wind
Air temperature (°C)	25-32	20-22	11-18
Water temperature (°C)	24 - 29	22 - 23	16 - 17
Maximum wind speed (m s⁻¹)	3.2	0.8	0.9
PHAR (mol m⁻² day⁻¹)	9.5	3.4	5.0
Secchi depth (cm)	15	30	40
TP (µg l⁻¹)	568	527	406
SRP (µg l⁻¹)	100	200	107
N-NH₄⁺ (µg l⁻¹)	23	783	560
N-NO₃⁻ (µg l⁻¹)	14	23	46
Chl-<i>a</i> (µg l⁻¹)	456	156	185
Phytoplankton composition	Cyanobacteria	Cyanobacteria, green algae, cryptophytes	Cryptophytes, green algae

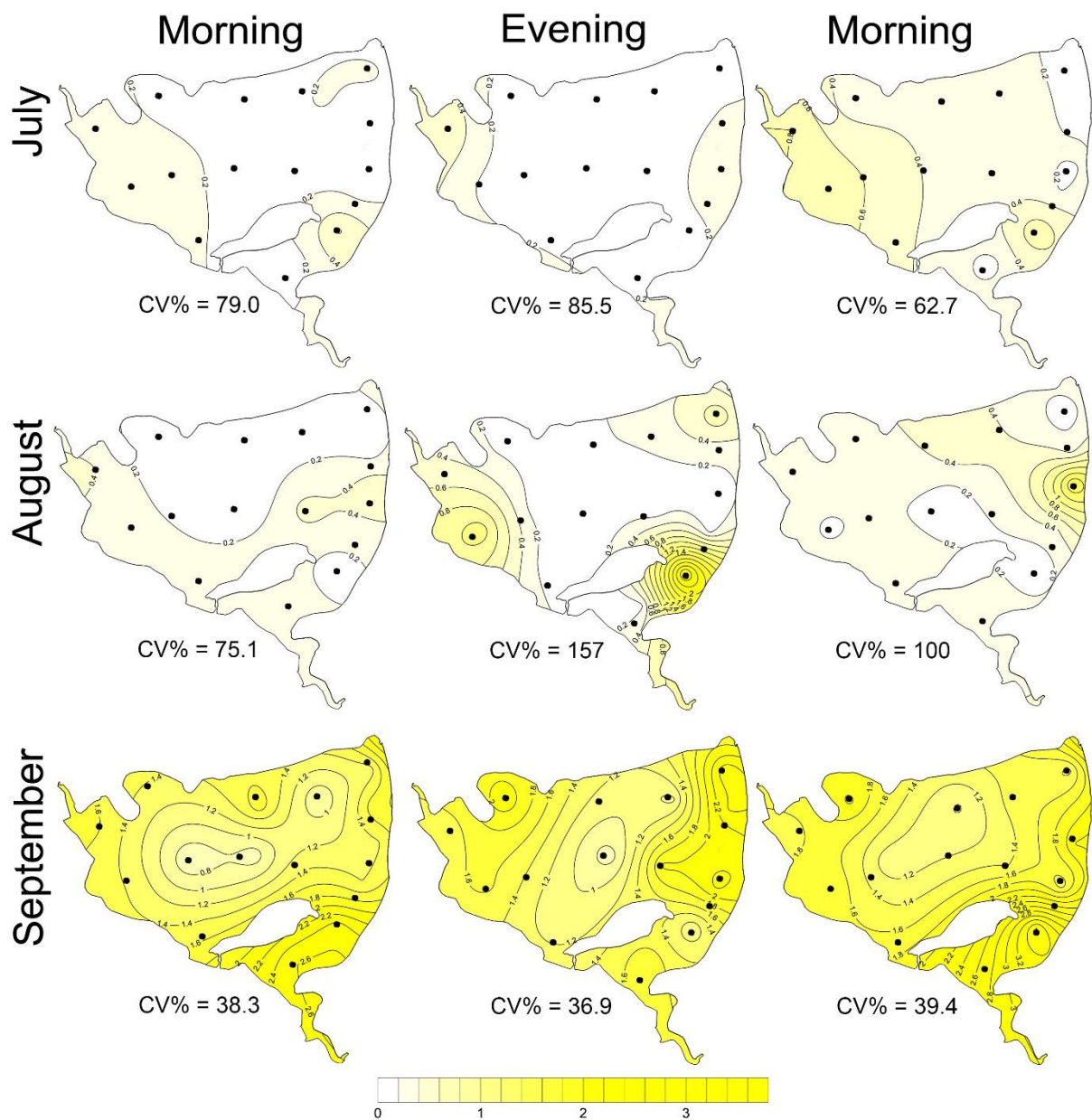
197
 198 Chlorophyll-*a* concentrations were highest in July due to the dense cyanobacterial bloom accumulated at the
 199 surface (Table 1). The phytoplankton consisted of only three cyanobacterial taxa: *Dolichospermum flos-aquae*,
 200 *Planktothrix agardhii*, and *Raphidiopsis mediteranea*. In August, phytoplankton was more diverse but also
 201 dominated by cyanobacteria: *P. agardhii*, *Aphanizomenon issatschenkoi*, and *D. flos-aquae*. In September,

202 cyanobacteria were absent and instead, cryptophytes (*Cryptomonas reflexa*), green algae (*Pediastrum*, *Coelastrum*
203 and *Desmodesmus*) and dinoflagellates (*Ceratium hirundinella*) prevailed.

204 3.2 Methane concentration and fluxes

205 The CH₄ concentration in surface water was highly supersaturated over the whole studied period. The obtained
206 values varied from 0.003 up to 3.75 μmol L⁻¹ (Fig. 2), which corresponded to saturation levels of 108-12 834%. It
207 is obvious, that the obtained data show remarkable variance: the mean (± SD) values were 0.22 ± 0.18 for July,
208 0.34 ± 0.45 for August, and 1.61 ± 0.61 μmol L⁻¹ for September (Suppl. Fig. 11).

209

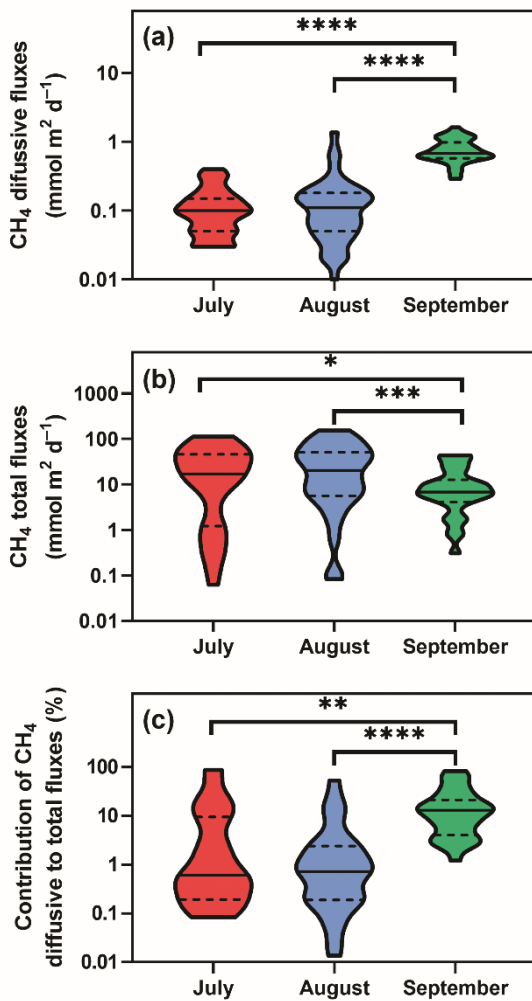


210

211 **Figure 2:** Surface methane concentrations (μmol L⁻¹). Contour graphs illustrating both seasonal and daily changes in spatial
212 heterogeneity (indicated by the coefficient of variation, CV%) in the fishpond. Black dots representing the sampling sites.

213

214 Diffusive fluxes (i.e., calculated from CH₄ concentration, see Eq. 2) showed the lowest values in July and August
215 (average 0.12 and 0.16 mmol m⁻² d⁻¹, respectively) and pronouncedly peaked in September (average 0.78 mmol
216 m⁻² d⁻¹, Fig. 3a). By contrast, in July and August, the average total CH₄ fluxes (obtained with floating chambers)
217 showed the highest values (average 31.8 mmol m⁻² d⁻¹; ranging from 0.08 to 152 mmol m⁻² d⁻¹) while in
218 September, total CH₄ fluxes were three times lower than before (average 11.8 mmol m⁻² d⁻¹, range 0.3 to 43.5
219 mmol m⁻² d⁻¹, Fig 3b). As a result, diffusive fluxes accounted for only a minor fraction of total CH₄ fluxes to the
220 atmosphere (on average, 9.2 % in July, 4.1 % in August, 18.5 % in September, Fig. 3c).



221

222 **Figure 3:** Violin plots of CH₄ diffusive (a) and total fluxes (b) during the studied period. Panel (c) depicts differences in the
223 percentage contribution of diffusive to total fluxes. Solid lines are medians, while dashed lines denote quartiles. Asterisks
224 indicate significant differences (* p<0.05, ** p<0.01, *** p<0.001, **** p<0.0001) between sampling dates determined by
225 two-way ANOVA with Tukey's multiple comparison test. Note that a log scale is used here for clarity.

226

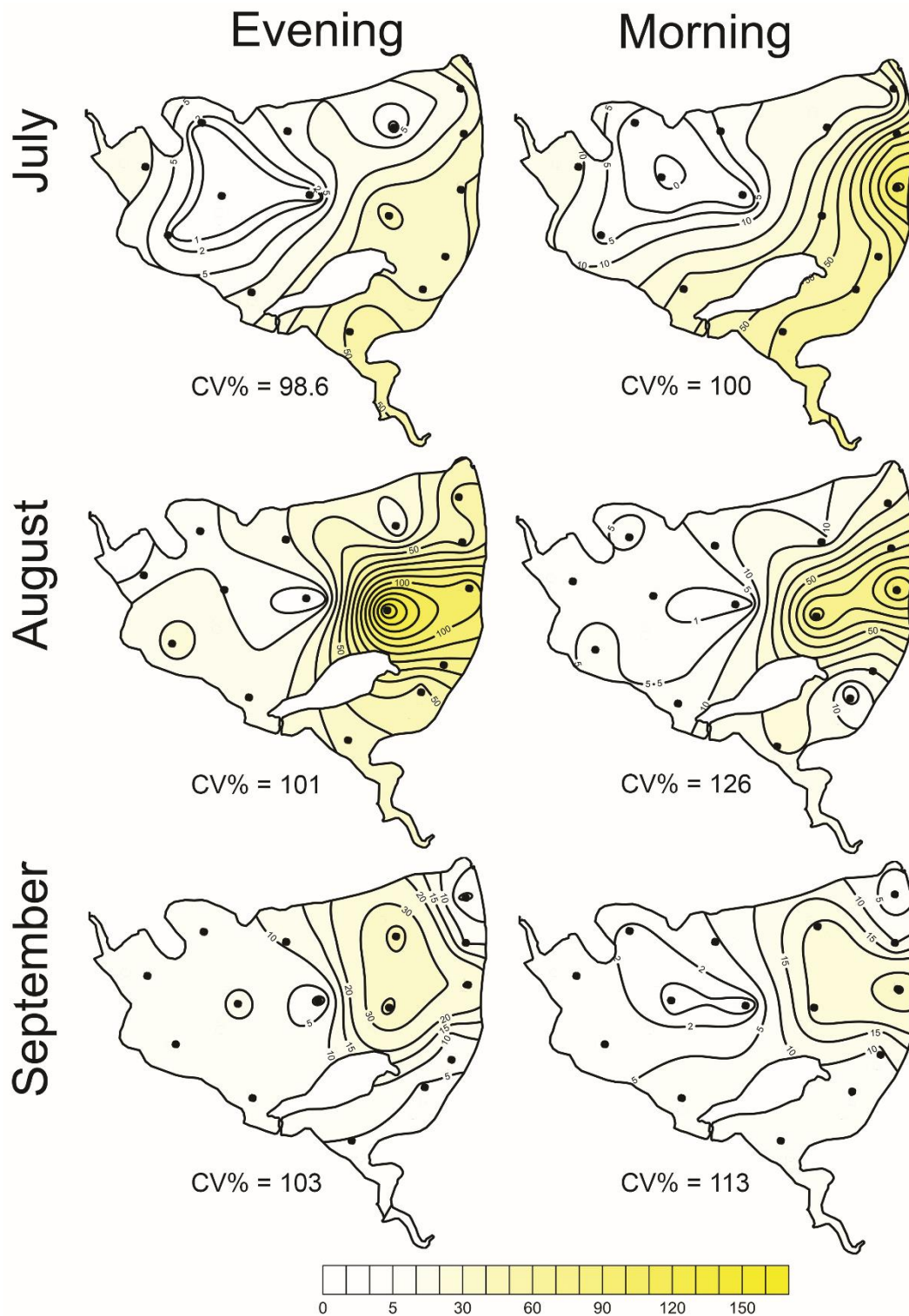
227 The total CH₄ fluxes show spatial variability within the fishpond that range four orders of magnitude (Fig. 3, 4;
228 Suppl. Fig. 11; Suppl. Table 1). The observed spatial pattern showed high temporal variability on both daily and

229 monthly scales (Fig. 2, 4, Suppl. Table 1). Most of the variability in CH₄ diffusive fluxes was explained by
 230 sampling date (62.4 %), while for the total CH₄ fluxes, spatial heterogeneity accounted for 87.2 % of data
 231 variability (Table 2). Using linear mixed-effects models, we identified water depth as the only significant predictor
 232 of total CH₄ fluxes (Df = 1, p < 0.0001, marginal Nakagawa's R² = 0.348; Fig. 5).

233 **Table 2:** The percentage of data variability explained by different factors (daytime, month = sampling date, and site)
 234 calculated with the Two-way RM ANOVA. Statistical significant values (p < 0.01) are bold.

	% of variability				Significance		
	Daytime	Month	Site	Unexplained	Daytime	Month	Site
CH₄ diffusive flux	2.3	62.4	13.2	22.1	0.0123	<0.0001	<i>n.s.</i>
CH₄ total flux	0.19	2.4	87.2	10.2	<i>n.s.</i>	<i>n.s.</i>	<0.0001
pH	4.4	64.9	11.1	19.6	0.0001	<0.0001	<i>n.s.</i>
Water temperature	3.3	92.3	2.5	1.9	<0.0001	<0.0001	<0.0001
O₂	21.7	48.1	13.8	16.4	<0.0001	<0.0001	0.0135
Chl-<i>a</i>	0.019	74.9	16.7	8.4	<i>n.s.</i>	<0.0001	<0.0001

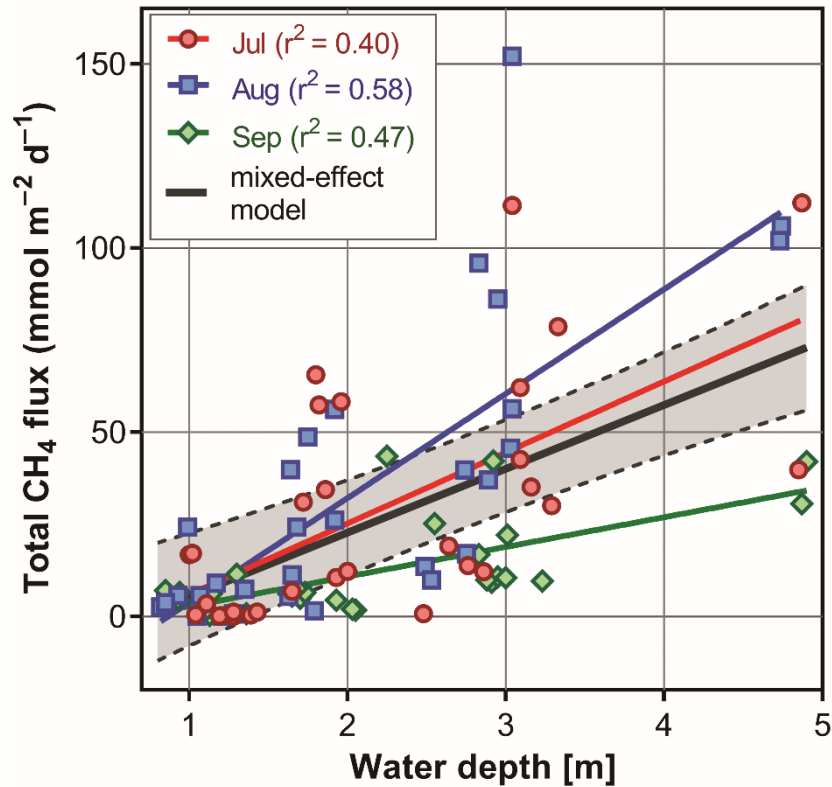
235 Interestingly, slopes of the linear regressions differed significantly among individual sampling campaigns (Fig. 5),
 236 indicating an additional season-related factor that affects CH₄ fluxes in the fishpond. Calculated CH₄ diffusive
 237 fluxes were not correlated with total fluxes. Linear mixed-effects models did not identify any significant predictor
 238 of the fluxes, indicating that factors and processes out of the study's scope are involved. We found no significant
 239 difference in either diffusive or total CH₄ fluxes between day and night.



240

241 **Figure 4:** Contour graphs of methane total fluxes in the Dehtář fishpond. Isopleths connect sites with the same value of
 242 methane fluxes ($\text{mmol m}^{-2} \text{day}^{-1}$). CV% is a measure of spatial heterogeneity. Black dots representing the sampling sites.

243

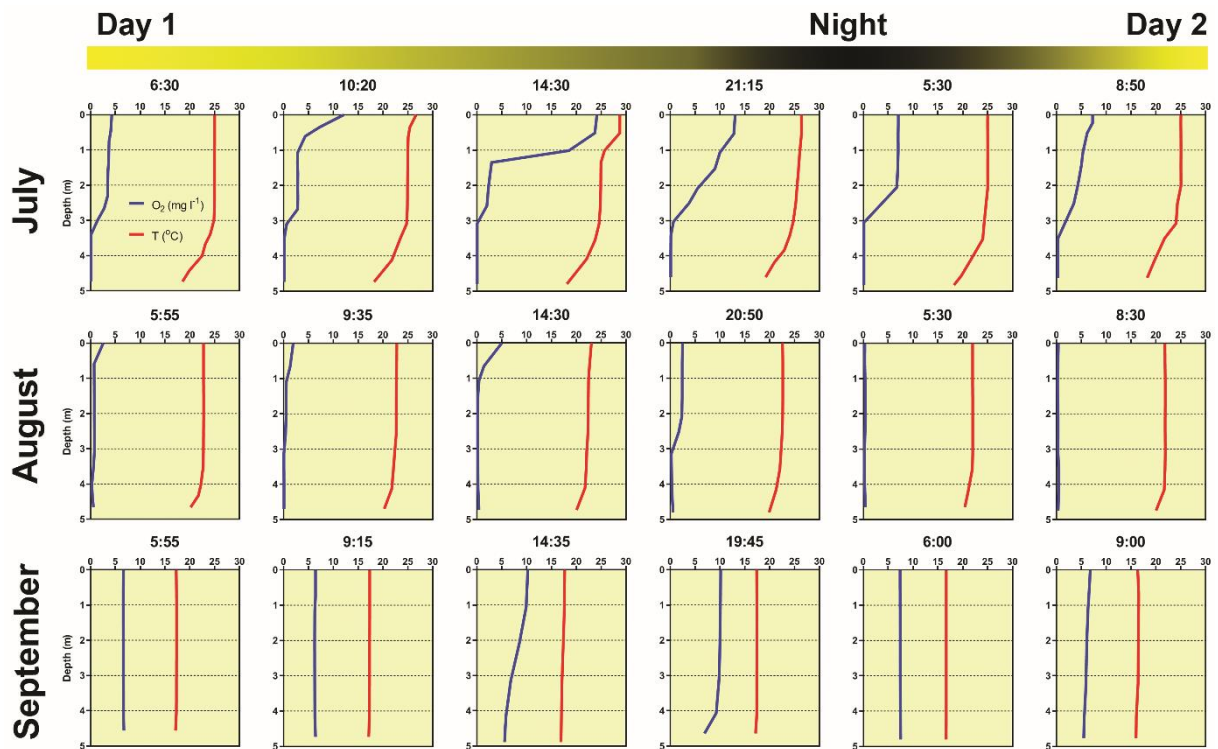


244

245 **Figure 5:** The most parsimonious linear mixed-effect model of methane total fluxes showing the water depth as the only
 246 significant predictor. Symbols are the measured values, the solid black line is the prediction, and dashed lines are 95th
 247 confidence intervals. Colours indicate month specific relation between total methane fluxes and water depth. Differences in
 248 slopes were tested using the F-test. In September, the slope of the regression line was significantly different from that in July
 249 and August.

250 3.3 Diurnal changes in vertical profiles of oxygen and temperature

251 Several contrasting patterns of vertical temperature and oxygen profiles occurred during summer 2019. Diurnal
 252 changes were most pronounced in July (Fig. 6). Surface temperatures varied from 25 °C in the morning to nearly
 253 30 °C in the afternoon. Thermal stratification of the water column was weak in the morning but became strongest
 254 at 14:30 with a thermocline at 0.5 m depth (Fig. 6). Later in the afternoon, the water column began to be mixed by
 255 wind. The morning vertical oxygen profile was characterised by a surface value of 4.3 mg L⁻¹, corresponding to
 256 51 % saturation and anoxia below 3 m.



257

258 **Figure 6:** Diurnal changes in vertical profiles of temperature and oxygen concentration measured at the deepest point of the
 259 fishpond. Numbers above each graph indicate the time of measurement.

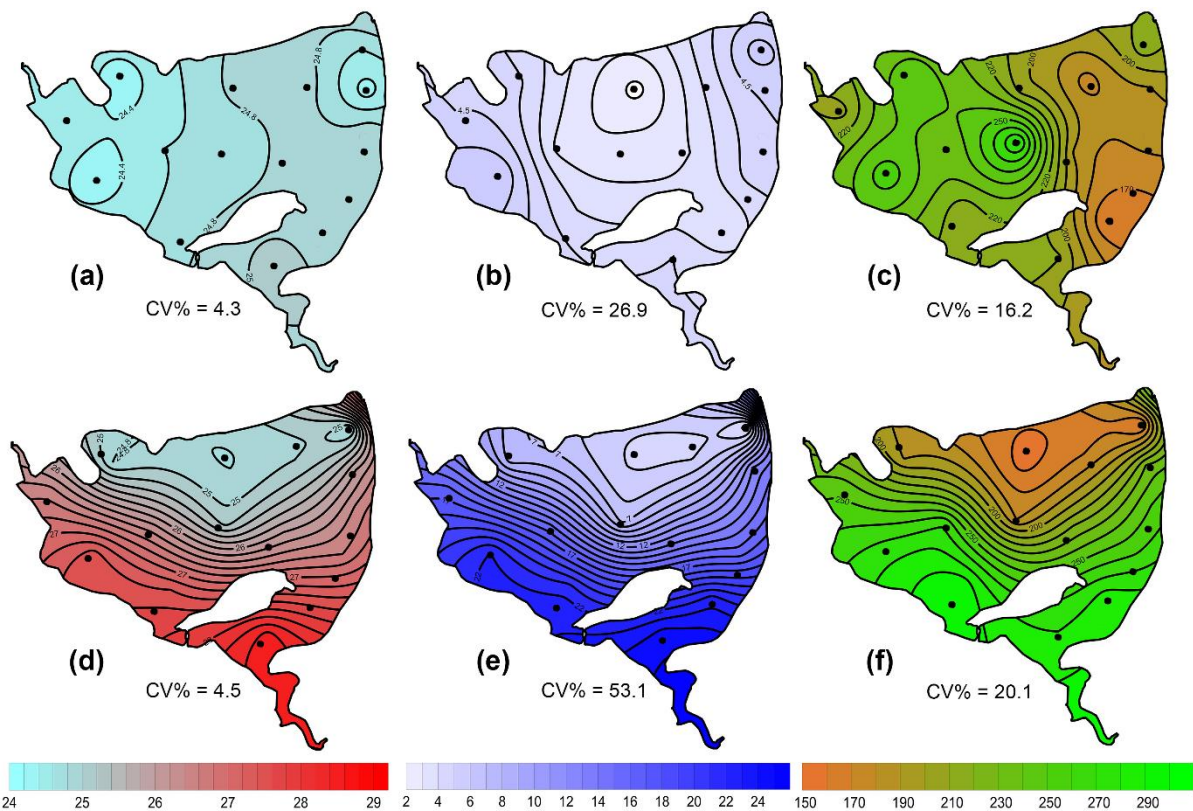
260 Due to the high photosynthetic activity of cyanobacteria, the surface oxygen concentration increased to 24 mg L^{-1}
 261 1 (320 % saturation, Fig. 6), and a steep oxycline was established at a depth of 0.5-1.5 m with no effect on the
 262 anoxic conditions at the deeper layers. Wind action eroded both the oxy- and thermoclines in the evening, and by
 263 the next morning, the vertical profiles were similar to those at the beginning.

264 In August, the water column was almost entirely mixed and low in oxygen in the morning, with only 2.6 mg L^{-1}
 265 (30 % saturation) of oxygen at the surface. Due to cloudy weather, the daily photosynthetic activity of
 266 phytoplankton resulted in only a slight increase in oxygen concentration at 0-1.5 m depth (4 mg L^{-1} , 47 %
 267 saturation). By the morning of the next day, the entire water column turned very close to anoxic (0.4 mg L^{-1} , 4 %
 268 saturation; Fig. 6), which in turn affected the spatial distribution of zooplankton, as evidenced by the formation of
 269 dense zooplankton clouds accumulated in the thin layer just at the surface (see Suppl. Fig. 3). In September, the
 270 water column was completely mixed, and we observed only weak daily changes in thermal and oxygen vertical
 271 structures (Fig. 6).

272 3.4 Effect of wind on spatial heterogeneity of temperature, oxygen and chlorophyll-*a*

273 During the summer, all measured parameters showed remarkable within-lake spatial heterogeneity (Suppl. Fig. 5-
 274 8). In July, meteorological conditions allowed for demonstrating the effect of wind on fishpond spatial

275 heterogeneity. In the morning, there were no substantial differences in the surface temperature and oxygen
 276 concentrations (Fig. 7ab). Phytoplankton biomass was accumulated mostly in the shallow western part, with the
 277 maximum in the centre (Fig. 7c). At 14:00, a light breeze started to blow from the northwest, achieving a maximum
 278 of 3.2 m s^{-1} (Suppl. Fig. 9). This episode lasted till the evening measurement, and the wind ceased by 21:00. The
 279 wind was strong enough to change spatial distribution substantially (Fig. 7d-f, Suppl. Fig. 4). In the evening, the
 280 surface water temperature on the windward (south) side of the fishpond was $\sim 4 \text{ }^\circ\text{C}$ higher than in the north (Fig.
 281 7d). The wind also induced order of magnitude differences in oxygen concentration along the north-south axis of
 282 the fishpond (3 mg L^{-1} of O_2 at the north, 24 mg L^{-1} of O_2 at the south; Fig. 7e) and affected phytoplankton
 283 distribution in the fishpond, resulting in remarkable bloom accumulation in the south (Fig. 7f, Suppl. Fig. 8).
 284 During the calm night after the disturbance, the north-south gradient substantially weakened. In August and
 285 September, the thermal heterogeneity of the pond was rather low, but the spatial distribution of oxygen and
 286 chlorophyll-*a* remained highly variable (Suppl. Fig. 5–8, Suppl. Table 1).



287
 288 **Figure 7:** Contour graphs of surface temperature (a, d; $^\circ\text{C}$), oxygen concentration (b, e; mg L^{-1}) and chlorophyll-*a*
 289 concentration (c, f; $\mu\text{g L}^{-1}$) measured on July 2 at different times of day: a, b and c are the morning measurements; d, e and f
 290 are evening measurements following a wind disturbance. Coefficient of variation (CV %) is a measure of spatial heterogeneity
 291 of measured parameters. Black dots representing the sampling sites.

292 **Discussion**

293 **4.1 Methane fluxes**

294 Assessing spatial heterogeneity of the CH₄ fluxes within a fishpond is critical for a reliable estimate of its
295 contribution to the global CH₄ budget. In our study, the variability in total CH₄ fluxes spanned several orders of
296 magnitude (ranging from 0.06 up to 1 121.3 mmol m⁻² d⁻¹), which is in agreement with similar studies (Casper et
297 al., 2000; DelSontro et al., 2016; Natchimuthu et al., 2016). However, most system-specific CH₄ flux estimates rely
298 on upscaling from a limited number of sites (Bastviken et al., 2004; Rasilo et al., 2015; Wik et al., 2016) because
299 obtaining spatial variability in CH₄ emission is methodologically challenging. In general, spatial heterogeneity
300 may reflect differences in water sources, physical mixing, local transformations and biogeochemical processes and
301 rates among lake habitats (Loken et al., 2019). In deep lakes, littoral areas can contribute disproportionately to
302 total lake CH₄ fluxes (Hofmann et al., 2010; Hofmann 2013, Natchimuthu et al., 2016; Schilder et al., 2013) and
303 are often missed by traditional sampling approaches (Wik et al., 2016). According to Wik et al. (2016), low
304 temporal and spatial resolutions are unlikely to cause overestimates. On the other hand, DelSontro et al. (2018b)
305 suggested that horizontal transport of CH₄ produced in littoral zones and the interaction between physical and
306 biological processes (e.g. air-water gas exchange, water column mixing, the interplay between CH₄ production
307 and microbial oxidation) may result in an underestimation of whole-lake CH₄ fluxes based on centre samples.
308 Similarly, Natchimuthu et al. (2016) found that up to 78 % underestimation would occur if samples obtained only
309 from the lake center are used to extrapolate the total CH₄ flux. However, extrapolating our data from the deepest
310 point of the Dehtář fishpond would lead to an overestimation of the CH₄ fluxes by a factor of 2.9 (Suppl. Fig. 12).
311 The bias introduced by the deepest point measurement appears to be highly variable among systems with different
312 morphology, geographical location, mixing regimes or trophic states. For instance, analysis of 22 European lakes
313 during late summer has shown that spatially resolved CH₄ diffusive fluxes were highly variable for individual
314 lakes, yielding 55–300 % differences in the whole-lake estimates (Schilder et al., 2013). Schmiedeskamp et al.
315 (2021) observed an increase in CH₄ fluxes from the shore towards the centre in response to increasing sediment
316 C-content in two shallow German lakes. In line with these findings, our results provide further evidence that
317 spatially resolved data are needed to validate the uncertainties that come from using single-point samples to
318 represent whole-lake processes in hyper-eutrophic systems. As stated by Loken et al. (2019), rather than assuming
319 spatial homogeneity, scaling-up exercises of global carbon budgets should acknowledge the uncertainty that comes
320 from extrapolating from spatially limited data sets.

321 In the Dehtář fishpond, the total CH₄ fluxes increased with water depth, and this relationship was month specific.
322 The highest CH₄ fluxes at the deepest points may seem contradictory to previous studies, in which the highest
323 fluxes were typically observed in littoral areas (e.g. DelSontro et al., 2018b; Hofman et al., 2010; Natchimuthu et
324 al., 2016; Schilder et al., 2013). However, these findings are based on studying mostly lakes whose morphology,
325 trophic state or oxygen regime sharply contrast with the Dehtář fishpond, where the upper two meters of the water
326 column were oxygen-saturated while the deepest strata were mostly anoxic, i.e. the extent and duration of bottom
327 anoxia could be the most influential factor contributing to the highest methane fluxes at the deepest point of the
328 pond. In such hyper-eutrophic systems, high nutrient loading increases autochthonous primary production
329 (Potužák et al., 2007; Rutegwa et al., 2019) and promotes oxygen consumption and anaerobic decomposition in
330 the sediments (Baxa et al., 2020), leading to enhanced CH₄ production (Bastviken et al., 2004; Grasset et al., 2018).
331 In aquaculture ponds in Southeast China, CH₄ fluxes exhibited considerable spatial variations and peaked in the
332 relatively deep feeding zone, where the large loads of sediment organic matter fueled CH₄ production (Yang et al.,
333 2020). Furthermore, sediment temperature was the strongest predictor of CH₄ fluxes in ponds (DelSontro et al.,
334 2016; Yang et al., 2020). It is, therefore, reasonable to assume that both temperature and oxygen concentration in
335 the sediment likely contributed to changes in observed CH₄ fluxes during the studied period in our study. Although
336 both parameters were not directly measured in the sediment, it can be deduced from their vertical profiles that the
337 probability of sediment anoxia was highest in August and lowest in September, and the sediment temperature was
338 lowest in September (see Fig. 5).

339 Our results agree with the generally accepted view that processes other than diffusive fluxes – most likely
340 ebullition – represent the major CH₄ pathway to the atmosphere in hyper-eutrophic ponds (Kosten et al., 2020).
341 Although freshwaters with high primary production are more likely to have high CH₄ ebullition rates (DelSontro
342 et al., 2016), the dominant role of ebullition was also found across lentic systems differing in size, trophic status
343 or geographical location (Aben et al., 2017). Ebullition accounted on average for 56 % of total CH₄ fluxes in
344 northern ponds in Canada (DelSontro et al., 2016), 49 and 71 % in two different zones of Lake Taihu (Xiao et al.,
345 2017) and 48-83 % in three Swedish lakes (Natchimuthu et al., 2016; Jansen et al., 2019). The highest contribution
346 was found in the small hyper-eutrophic Priest Pot (UK), where ebullition represented 96 % of the total CH₄ flux
347 from the pond (Casper et al., 2000). Apparently, the contribution of ebullition can vary among systems and will
348 remain uncertain until measurement designs cover enough spatiotemporal variability to yield representative values
349 for the whole ecosystem.

350 In shallow water bodies, a semi-stable flux of microbubbles was suggested to account for a significant portion of
351 the total CH₄ flux (Prairie and del Giorgio, 2013). When CH₄ concentration in the water column is above a certain
352 threshold of microbubble density, these microbubbles likely aggregate, fuse, and escape to the atmosphere from
353 buoyancy (Prairie and del Giorgio, 2013). Even a small fluctuation in hydrostatic pressure (e.g., due to changes in
354 atmospheric pressure) or lake water level was shown to trigger enhanced CH₄ ebullition (Bastviken et al., 2004;
355 Casper et al., 2000; Varadharajan and Hemond, 2012). Since ebullition rates increase exponentially with
356 temperature, CH₄ fluxes tend to peak in warm summer months (van Bergen et al., 2019). In our study, 1 % lower
357 air pressure in July and August than in September, along with bottom anoxia and higher water temperature, could
358 account for the enhanced release of CH₄ bubbles from the sediment (31.7 mmol m⁻²d⁻¹, >90 % of total CH₄ fluxes;
359 Suppl. Fig. 2). In September, when we observed the lowest water temperatures from the studied period and the
360 oxygen profile was rather uniform, ebullition accounted for 81 % (11 mmol m⁻²d⁻¹) of the total CH₄ fluxes. The
361 spatially pooled data of the total CH₄ fluxes measured in the Dehtář fishpond varied from 11.8 to 34.5 mmol m⁻²
362 d⁻¹, which is comparable with similar systems elsewhere (e.g., Bastviken et al., 2010; van Bergen et al., 2019;
363 Baron et al., 2022). To sum up, both diffusive fluxes and ebullition must be addressed to understand the magnitude
364 of total aquatic CH₄ fluxes and how their relative contributions vary across and within aquatic systems (Kosten et
365 al., 2020). Moreover, with an improved determination of CH₄ hot-spots and its causes, the management of ponds
366 could be changed accordingly and so the overall emissions reduced for example by decreasing P-availability and
367 dredging (Nijman et al., 2022).

368 **4.2 Effect of wind event on ecosystem spatial structure**

369 Sudden changes in ecosystem spatial structure in response to meteorological forcing have rarely been documented
370 (Loken et al., 2019) since they are hard to predict. Research into them using traditional methods requires intensive
371 effort or expensive instrumentation (Ortiz and Wilkinson, 2021), and it remains a matter of luck to obtain a relevant
372 dataset. In the July sampling campaign, we observed a strong impact of the wind on environmental heterogeneity
373 in the fishpond, which was apparent at a sub-daily time scale. Due to the methodological constraints, i.e., lack of
374 initial measurement, we can only speculate about the effect of wind on the total CH₄ fluxes. The northwest wind
375 during the day advected warmed surface water with cyanobacterial bloom from the north basin to the south. In the
376 evening, it resulted in bloom accumulation on the upward side and a north-south gradient of more than 4 °C and
377 4-24 mg L⁻¹ oxygen. After the winds fell off, the observed gradients declined during cooling at night. We assume
378 that the wind blowing across the pond surface drove buoyant cyanobacteria and surface water downwind and
379 caused an upwelling of deeper, colder, and hypoxic water on the upwind side. This wind-related circulation pattern

380 has been described as a “conveyer belt” in classical textbooks (Reynolds et al., 2006), held responsible for a
381 disruption of the thermal structure of the water column and the non-uniform spatial distribution of pH, oxygen,
382 CO₂ or CH₄ and also plankton assemblages (e.g. Loken et al., 2019; Natchimuthu et al., 2016; Rinke et al., 2009;
383 Ortiz and Wilkinson, 2021).

384 Similar to our study, mild winds (~4 m s⁻¹) were strong enough to redistribute heat and induce lake-wide
385 circulations driving upwelling and downwelling in 24 m deep Lake Pleasant (Czikowsky et al., 2018). As the wind
386 blows harder and lasts longer, the effects on ecosystem functioning may target higher trophic levels and become
387 more complex (Rinke et al., 2009). In Lake Constance, a three day storm event with wind velocities of ~10 m s⁻¹
388 resulted in a lake-wide displacement of water masses and the formation of the 6-15 °C horizontal surface water
389 gradient, which in turn changed the spatial distribution of phytoplankton, zooplankton and juvenile fish (Rinke et
390 al., 2009). After several stormy days (wind velocities of 12-15 m s⁻¹), Čech et al. (2011) observed negative effects
391 of wind-driven changes in water temperature and wave action on perch (*Perca fluviatilis*) spawning in the Lake
392 Milada. Although wind events affect shallow and deep lakes differently, there is growing evidence that they can
393 have far-reaching consequences on the functioning of aquatic ecosystems by disrupting energy flows, nutrient
394 fluxes, productivity and reproduction, and consequently altering community composition and trophic interactions
395 in the short and long term (Stockwell et al., 2020). As the frequency, intensity, spatial extent and duration of these
396 extreme meteorological events are projected to increase due to ongoing climate change (Comou and Rahmstorf,
397 2012), there is an urgent need to better understand the mechanisms underlying their impacts on the maintenance
398 of the ecosystem services.

399 **4.3 Summer changes in the oxygen regime**

400 Our data demonstrate that shallow, hyper-eutrophic ponds have disrupted oxygen regimes (Baxa et al., 2021) with
401 anoxic hypolimnion and may experience severe whole-water column hypoxia critical for aquatic biota (Miranda
402 et al., 2001). The hypoxic periods may result, for example, from sudden weather change (Jeppesen et al., 1990)
403 and last several days, during which physical processes and phytoplankton photosynthesis cannot compensate for
404 intense community respiration (Baxa et al., 2021). This became obvious in August when severe oxygen depletion
405 was measured at the surface across the whole pond, mostly far below a critical level of 4.5 mg L⁻¹, when adverse
406 effects came into play (Banerjee et al., 2019). However, oxygen surface concentrations in shallow parts of the
407 pond were substantially higher regardless of the time of day, which contrasts with findings of Miranda et al. (2001),
408 who emphasised shallow waters as the most sensitive parts of lakes, where hypoxic events can occur due to the
409 respiration of sediment biota. The observed spatial gradients of oxygen may create temporal refugia which allow

410 fish to survive harsh conditions that occur in the deepest part of the pond. To minimise economic losses and
411 negative impacts on the ecosystem, future research should identify the interplay between meteorological forcing,
412 trophic status and anthropogenic pressures (e.g. management practices) that affect oxygen fluctuations at various
413 time scales.

414 **4.4 Study limitations**

415 Like in other research, there are some limitations in the current study. Since our measurement had only a limited
416 temporal resolution (three samplings during the summer season), it is not appropriate to extrapolate CH₄ emissions
417 for annual values. Noticeably, future research must increase the frequency of the sampling and include also
418 innovative techniques to measure CH₄ fluxes at multiple fishponds, with different management regime. In our
419 study, the 12 h deployment time of the floating chambers could have led to extensive gas accumulation, which in
420 turn might have resulted in an underestimation of the total CH₄ fluxes due to the dissolution of the CH₄ from the
421 chamber into the water once the equilibrium concentration in the chamber is overcome (Bastviken et al., 2010).
422 However, CH₄ concentrations in water corresponded to a supersaturation of several orders of magnitude, so the
423 introduced bias appears to be of minor importance. In any case, our daily CH₄ fluxes represent a rather conservative
424 estimate for the global methane budget. In our study, we also did not address the important processes that could
425 shed light on the lake CH₄ budget, such as CH₄ oxidation rates (Bastviken et al., 2008) or biological interaction
426 (e.g. protistan grazing on CH₄ oxidising bacteria) in aquatic food webs (Sanseverino et al., 2012) that can affect
427 the overall CH₄ fluxes. We also lack information about spatial differences in sediment microbiota and organic
428 carbon content and compositions, which were found to affect CH₄ production rates (Berberich et al., 2020;
429 Emerson et al., 2021). Despite the limitation mentioned above, our results show that complementary spatial
430 surveys help contextualise the fixed station dynamics and provide additional, management-relevant information
431 about the fishpond.

432 **For improved monitoring strategies, however, a continuous measurement approach like eddy covariance**
433 **would be generally more efficient than traditional sampling at regular intervals. Eddy covariance accounts**
434 **for temporal variability and provides high temporal resolution data by continuously measuring wind speed,**
435 **gas concentration, and vertical turbulent fluxes to estimate methane emissions (Erkillä et al., 2018). More**
436 **importantly, it also offers spatially integrated measurements, averaging emissions over a larger area and**
437 **therefore accounts for pond spatial heterogeneity. However, it's worth noting that the choice of monitoring**
438 **approach depends on various factors, including the specific objectives, available resources, and the**
439 **characteristics of the emission sources. To accurately capture both short-term variability and lake spatial**
440 **heterogeneity of methane ebullition and diffusion fluxes, the most efficient approach was found to be a**
441 **combination of continuous measurements with traditional methods including floating chambers, anchored**
442 **funnels and boundary model calculations (Schubert et al., 2012, Podgrajsek et al., 2014, Erkillä et al., 2018).**
443 **This integrated approach would provide a comprehensive understanding of methane emissions, enabling**
444 **better estimation and more effective mitigation efforts.**

445 Deciphering the mechanisms that drive spatial and temporal heterogeneity in aquatic ecosystem structure and
446 function not only expands our understanding of pond ecology but also provides insights to improve the
447 management of these ecosystems and the services they provide. Our results suggest that spatial heterogeneity needs
448 to be considered when designing experiments and monitoring programs. Without the spatially resolved sampling,
449 we introduce bias into our datasets, hampering our limnological understanding of the ecosystem's functioning and
450 impeding our ability to accurately estimate rates such as methane emissions on a global scale (DeISontro et al.,
451 2018a). In agreement with Kosten et al. (2020), we demonstrated that neglecting ebullition leads to a considerable
452 underestimating of the total CH₄ fluxes. Since there are thousands of these intensively managed fishponds, we
453 argue for changing the management practices toward sustainable use of natural resources to mitigate the overall
454 emissions of greenhouse gases from these ecosystems. Future studies are needed to characterise CH₄ fluxes over
455 a greater number and diversity of aquaculture ponds and examine the mechanisms controlling CH₄ emissions in
456 aquatic ecosystems.

457 **Acknowledgements**

458 The study was supported by the Czech Science Foundation (Research Projects No. 17-09310S, 19-23261S and
459 P504/19-16554S). We thank Dr. Martin Rulík for providing us gas chambers. We especially thank to Prof.
460 Miloslav Šimek and Linda Jišová for enabling gas analyses. We are grateful Anna Sieczko for consultation on the
461 calculation of CH₄ fluxes. English correction was made by Anton Baer.

462 **Data availability**

463 Dataset associated with the manuscript can be found in the GitHub Repositories under
464 <https://zenodo.org/badge/latestdoi/587640213>.

465 **Author contributions**

466 All authors contributed to the study conception and design. PZ planned the campaign; PZ, AM and JN performed
467 the sampling and analyzed the data; AM performed the gas-measurements; VK performed statistical analyses and
468 modelling; PZ and AM wrote the manuscript. All authors read and approved the final manuscript.

469 **References**

- 470 Aben, R.C.H., Barros, N., van Donk, E., Frenken, T., Hilt, S., Kazanjian, G., Lamers, L.P.M., Peeters, E.T.H.M.,
471 Roelofs, J.G. M, de Senerpont Domis, L.N., Stephan, S., Velthuis, M., Van de Waal, D.B., Wik, M., Thornton,
472 B.F., Wilkinson, J., DelSontro, T., and Kosten, S.: Cross continental increase in methane ebullition under climate
473 change. *Nat. Commun.*, 8, 1682, <https://doi.org/10.1038/s41467-017-01535-y>, 2017.
- 474 Banerjee, A., Chakrabarty, M., Rakshit, N., Bhowmick, A.R., and Ray, S.: Environmental factors as indicators of
475 dissolved oxygen concentration and zooplankton abundance: deep learning versus traditional regression approach.
476 *Ecol. Indic.*, 100, 99-117, <https://doi.org/10.1016/j.ecolind.2018.09.051>, 2019.
- 477 Baron, A.A.P., Dyck, L.T., Amjad, H., Bragg, J., Kroft, E., Newson, J., Oleson, K., Casson, N.J., North, R.L.,
478 Venkiteswaran, J.J., and Whitfield, C.J.: Differences in ebullitive methane release from small, shallow ponds
479 present challenges for scaling. *Sci. Total Environ.*, 802, 149685, <https://doi.org/10.1016/j.scitotenv.2021.149685>,
480 2022.
- 481 Bartosiewicz, M., Maranger, R., Przytulska, A., and Laurion, I.: Effects of phytoplankton blooms on fluxes and
482 emissions of greenhouse gases in a eutrophic lake. *Water Res.*, 196, 116985,
483 <https://doi.org/10.1016/j.watres.2021.116985>, 2021.
- 484 Bastviken, D., Cole, J., Pace M., and Tranvik, L.: Methane emissions from lakes: Dependence of lake
485 characteristics, two regional assessments, and a global estimate. *Global Biogeochem. Cycles*, 18, GB4009,
486 <https://doi.org/10.1029/2004GB002238>, 2004.
- 487 Bastviken, D., Cole, J.J., Pace, M.L., and Van de Bogert, M.C.: Fates of methane from different lake habitats:
488 connecting whole-lake budgets and CH₄ emissions. *J. Geophys. Res. Biogeosci.*, 113, G02024,
489 <https://doi.org/10.1029/2007JG000608>, 2008.
- 490 Bastviken, D., Santoro, A.L., Marotta, H., Pinho, L.Q., Calheiros, D.F., Crill, P., and Enrich-Prast, A.: Methane
491 Emissions from Pantanal, South America, during the Low Water Season: Toward More Comprehensive Sampling.
492 *Environ. Sci. Tech.*, 44, 5450-5455, <https://doi.org/10.1021/es1005048>, 2010.
- 493 Bates, D., Maechler, M., Bolker, B., and Walker, S.: Fitting Linear Mixed-Effects Models Using lme4. *J. Stat.*
494 *Soft.*, 67, 1-48, <https://doi.org/10.18637/jss.v067.i01>, 2015.
- 495 Baxa, M., Musil, M., Kummel, M., Hazlík, O., Tesařová, B., and Pechar, L.: Dissolved oxygen deficits in a shallow
496 eutrophic aquatic ecosystem (fishpond) – Sediment oxygen demand and water column respiration alternately drive
497 the oxygen regime. *Sci. Total Environ.*, 766, 142647, <https://doi.org/10.1016/j.scitotenv.2020.142647>, 2021.
- 498 Berberich, M.E., Beaulieu, J.J., Hamilton, T.L., Waldo, S., and Buffam, I.: Spatial variability of sediment methane
499 production and methanogen communities within a eutrophic reservoir: Importance of organic matter source and
500 quantity. *Limnol. Oceanogr.*, 65, 1336-1358, <https://doi.org/10.1002/lno.11392>, 2020.

501 Bižić, M., Klintzsch, T., Ionescu, D., Hindiyeh, M.Y., Günthel, M., Muro-Pastor, A.M., Eckert, W., Urich, T.,
502 Keppler, F., and Grossart, H.P.: Aquatic and terrestrial cyanobacteria produce methane. *Sci. Adv.*, 6, 1-10,
503 <https://doi.org/10.1126/sciadv.aax5343>, 2020.

504 Bussmann, I., Matoušů, A., Osudar, R., and Mau, S.: Assessment of the radio $^3\text{H-CH}_4$ tracer technique to measure
505 aerobic methane oxidation in the water column. *Limnol. Oceanogr.- Meth.*, 13, 312-327,
506 <https://doi.org/10.1002/lom3.10027>, 2015.

507 Casper, P., Maberly, S.C., Hall, G.H., and Finlay, B.J.: Fluxes of methane and carbon dioxide from a small
508 productive lake to the atmosphere. *Biogeochemistry*, 49, 1-19, <https://doi.org/10.1023/A:1006269900174>, 2000.

509 Čech, M., Peterka, J., Říha, M., Muška, M., Hejzlar, J., and Kubečka, J.: Location and timing of the deposition of
510 eggs strands by perch (*Perca fluviatilis* L.): the roles of lake hydrology, spawning substrate and female size.
511 *Knowl. Manag. Aquat. Ecosyst.*, 403, 1-12, <https://doi.org/10.1051/kmae/2011070>, 2011.

512 Céréghino, R., Biggs, J., Oertli, B., and Declerck, S.: The ecology of European ponds: defining the characteristics
513 of a neglected freshwater habitat. *Hydrobiologia*, 597, 1-6, <https://doi.org/10.1007/s10750-007-9225-8>, 2008.

514 Coumou, D. and Rahmstorf, S.: A decade of weather extreme. *Nat. Clim. Change*, 2, 491-96,
515 <https://doi.org/10.1038/nclimate1452>, 2012.

516 Crusius, J. and Wanninkhof, R.: Gas transfer velocities measured at low wind speed over a lake. *Limnol. Oceanogr.*,
517 48, 1010-1017, <https://doi.org/10.4319/lo.2003.48.3.1010>, 2003.

518 Czikowsky, M.J., MacIntyre, S., Tedford, E.W., Vidal, J., and Miller, S.D.: Effects of wind and buoyancy on
519 carbon dioxide distribution and air-water flux of a stratified temperate lake. *J. Geophys. Res. Biogeosci.*, 123,
520 2305-2322, <https://doi.org/10.1029/2017JG004209>, 2018.

521 De Meester, L., Declerck, S., Stoks, R., Louette, G., Van de Meutter, F., De Bie, T., Michels, E., and Brendonck,
522 L.: Ponds and pools as model systems in conservation biology, ecology and evolutionary biology. *Aquat. Cons.*,
523 15, 715-725, <https://doi.org/10.1002/aqc.748>, 2005.

524 DelSontro, T., Boutet, L., St-Pierre, A., del Giorgio, P.A., and Prairie, Y.T.: Methane ebullition and diffusion from
525 northern ponds and lakes regulated by the interaction between temperature and system productivity. *Limnol.*
526 *Oceanogr.*, 61, 62-77, <https://doi.org/10.1002/lno.10335>, 2016.

527 DelSontro, T., Beaulieu, J.J., and Downing, J.J.: Greenhouse gas emissions from lakes and impoundments:
528 upscaling in the face of global change. *Limnol. Oceanogr. Lett.*, 3, 64-75, <https://doi.org/10.1002/lo12.10073>,
529 2018a.

530 DelSontro, T., del Giorgio, P.A., and Prairie, Y.T.: No Longer a Paradox: The Interaction Between Physical
531 Transport and Biological Processes Explains the Spatial Distribution of Surface Water Methane Within and Across
532 Lakes. *Ecosystems*, 21, 1073-1087, [10.1007/s10021-017-0205-1](https://doi.org/10.1007/s10021-017-0205-1), 2018b.

533 Emerson, J.B., Varner, R.K., Wik, M., Parks, D.H., Neumann, R.B., Johnson, J.E., Singleton, C. M., Woodcroft,
534 B.J., Tollerson II, R., Owusu-Domney, A., Binder, M., Freitas, N. L., Crill, P.M., Saleska, S.R., Tyson, G.W., and
535 Rich, V.I.: Diverse sediment microbiota shape methane emission temperature sensitivity in Arctic lakes. *Nat.*
536 *Commun.*, 12, 5815, <https://doi.org/10.1038/s41467-021-25983-9>, 2021.

537 Erkkilä, K.-M., Ojala, A., Bastviken, D., Biermann, T., Heiskanen, J. J., Lindroth, A., Peltola, O., Rantakari, M.,
538 Vesala, T., and Mammarella, I.: Methane and carbon dioxide fluxes over a lake: comparison between eddy
539 covariance, floating chambers and boundary layer method, *Biogeosciences*, 15, 429-445,
540 <https://doi.org/10.5194/bg-15-429-2018>, 2018.

541 Grasset, Ch., Mendonça, R., Saucedo, G.V., Bastviken, D., Roland, F., and Sobek, S.: Large but variable methane
542 production in anoxic freshwater sediment upon addition of allochthonous and autochthonous organic matter.
543 *Limnol. Oceanogr.*, 63, 1488-1501, <https://doi.org/10.1002/lno.10786>, 2018.

544 Halekoh, H. and Hojsgaard, S.: A Kenward-Roger Approximation and Parametric Bootstrap Methods for Tests in
545 Linear Mixed Models - The R Package pbrtest. *J. Stat. Soft.*, 59, 1-30, <https://doi.org/10.18637/jss.v059.i09> 2014.

546 Hofmann, H., Federwisch, L., and Peeters, F.: Wave-induced release of methane: littoral zones as a source of
547 methane in lakes. *Limnol. Oceanogr.*, 55, 1990-2000, <https://doi.org/10.4319/lo.2010.55.5.1990>, 2010.

548 Hofmann, H.: Spatiotemporal distribution patterns of dissolved methane in lakes: How accurate are the current
549 estimations of the diffusive flux path? *Geophys. Res. Lett.*, 40, 2779-2784, <https://doi.org/10.1002/grl.50453>,
550 2013.

551 Hu, Z., Wu, S., Ji, Ch., Zou, J., Zhou, Q., and Liu, S.: A comparison of methane emissions following rice paddies
552 conversion to crab-fish farming wetlands in southeast China. *Environ. Sci. Pollut. Res.*, 23, 1505-1515,
553 <https://doi.org/10.1007/s11356-015-5383-9>, 2016.

554 Jansen, J., Thornton, B.F., Jammot, M.M., Wik, M., Cortés, A., Friberg, T., MacIntyre, S., and Crill, P.M.:
555 Climate-sensitive controls on large spring emissions of CH₄ and CO₂ from northern lakes. *J. Geophys. Res.*,
556 *Biogeosciences*, 124, 2379-2399, <https://doi.org/10.1029/2019JG005094>, 2019.

557 Jähne, B., Münnich, K. O., Börsinger, R., Dutzi, A., Huber, W., and Libner, P.: On the parameters influencing air-
558 water gas exchange, *J. Geophys. Res.*, 92, C2, 1937-1949, doi:10.1029/JC092iC02p01937, 1987.

559 Jeppesen, E., Søndergaard, M., Sortkjaer, O., Mortensen, E., and Kristensen, P.: Interactions between
560 phytoplankton zooplankton and fish in a shallow hypertrophic Lake a study of phytoplankton collapses in Lake
561 Sobygaard, Denmark. *Hydrobiologia*, 1991, 149-164, <https://doi.org/10.1007/BF00026049>, 1990.

562 Kolar, V., Vlašánek, P., and Boukal, D.S.: The influence of successional stage on local odonate communities in
563 man-made standing waters. *Ecol. Eng.*, 173, 106440, <https://doi.org/10.1016/j.ecoleng.2021.106440>, 2021.

564 Kopáček, J. and Hejzlar, J.: Semi-micro determination of total phosphorus in fresh waters with perchloric acid
565 digestion. *Int. J. Environ. Anal. Chem.*, 53, 173-183, <https://doi.org/10.1080/03067319308045987>, 1993.

566 Kopáček, J. and Procházková, L.: Semi-Micro Determination of Ammonia in Water by the Rubazotic Acid Method.
567 *Int. J. Environ. Anal. Chem.*, 53, 243-248, <https://doi.org/10.1080/03067319308045993>, 1993.

568 Kosten, S., Almeida, R.M., Barbosa, I., Mendonça, R., Muzitano, I.S., Oliveira-Junior, E.S., Vroom, R.J.E., Wang,
569 H.J., and Barros, N.: Better assessments of greenhouse gas emissions from global fish ponds needed to adequately
570 evaluate aquaculture footprint. *Sci. Total Environ.*, 748, 141247, <https://doi.org/10.1016/j.scitotenv.2020.141247>,
571 2020.

572 Laas, A., Noges, P., Koiv, T., and Noges, T.: High-frequency metabolism study in a large and shallow temperate
573 lake reveals seasonal switching between net autotrophy and net heterotrophy. *Hydrobiologia*, 694, 57-74,
574 <https://doi.org/10.1007/s10750-012-1131-z>, 2012.

575 Loken, L.C., Crawford, J.T., Schramm, P.J., Stadler, P., Desai, A.R., and Stanley, E.H.: Large spatial and temporal
576 variability of carbon dioxide and methane in a eutrophic lake. *J. Geophys. Res. Biogeosci.*, 124, 2248-2266
577 <https://doi.org/10.1029/2019JG005186>, 2019.

578 Lüdecke, D.: "ggeffects: Tidy Data Frames of Marginal Effects from Regression Models." *J. Open Source Soft.*,
579 3, 772, <https://doi.org/10.21105/joss.00772>, 2018.

580 Lüdecke, D., Makowski, D., and Waggoner, P.: performance: Assessment of Regression Models Performance. R
581 package version 0.4.4. <https://CRAN.R-project.org/package=performance>, 2020.

582 Ma, Y., Sun, L., Liu, C., Yang, X., Zhou, W., Yang, B., Schwenke, G., and Liu, D.L.: A comparison of methane
583 and nitrous oxide emissions from inland mixed-fish and crab aquaculture ponds. *Sci. Total Environ.*, 637-638,
584 517-523, <https://doi.org/10.1016/j.scitotenv.2018.05.040>, 2018

585 McAuliffe, C.: Gas Chromatographic determination of solutes by multiple phase equilibrium. *Chem. Technol.*, 1,
586 46-51, 1971.

587 Miranda, L.E., Hargreaves, J.A., and Raborn, S.W.: Predicting and managing risk of unsuitable dissolved oxygen
588 in a eutrophic lake. *Hydrobiologia*, 457, 177-185, <https://doi.org/10.1023/A:1012283603339>, 2001.

589 Murphy, J. and Riley, J.P.: A modified single-solution method for the determination of phosphate in natural waters.
590 *Anal. Chim. Acta*, 27, 31-36, [https://doi.org/10.1016/S0003-2670\(00\)88444-5](https://doi.org/10.1016/S0003-2670(00)88444-5), 1962.

591 Natchimuthu, S., Sundgren, I., Gålfalk, M., Klemetsson, L., Crill, P., Danielsson, Å., and Bastviken, D.: Spatio-
592 temporal variability of lake CH₄ fluxes and its influence on annual whole lake emission estimates. *Limnol.*
593 *Oceanogr.*, 61, 13-26, <https://doi.org/10.1002/lno.10222>, 2016.

594 Nijman, T.P.A., Lemmens, M., Lurling, M., Kosten, S., Welte, C., and Veraart, A.J.: Phosphorus control and
595 dredging decrease methane emissions from shallow lakes. *Sci. Total Environ.*, 847, 15758,
596 <https://doi.org/10.1016/j.scitotenv.2022.157584>, 2022.

597 Ortiz, D.A. and Wilkinson, G.M.: Capturing the spatial variability of algal bloom development in a shallow
598 temperate lake. *Freshwater Biol.*, 66, 2064-2075, <https://doi.org/10.1111/fwb.13814>, 2021.

599 Pechar, L.: Impacts of long-term changes in fishery management on the trophic level and water quality in Czech
600 fishponds. *Fisheries Manag. Ecol.*, 7, 23-32, [10.1046/j.1365-2400.2000.00193.x](https://doi.org/10.1046/j.1365-2400.2000.00193.x), 2000.

601 Pokorný, J. and Hauser, V.: The restoration of fish ponds in agricultural landscapes. *Ecol. Eng.*, 18, 555-574,
602 [https://doi.org/10.1016/S0925-8574\(02\)00020-4](https://doi.org/10.1016/S0925-8574(02)00020-4), 2002.

603 Podgrajsek, E., Sahlée, E., Bastviken, D., Holst, J., Lindroth, A., Tranvik, L., and Rutgersson, A.: Comparison of
604 floating chamber and eddy covariance measurements of lake greenhouse gas fluxes, *Biogeosciences*, 11, 4225–
605 4233, <https://doi.org/10.5194/bg-11-4225-2014>, 2014.

606 Potužák, J., Hůda, J., and Pechar, L.: Changes in fish production effectivity in eutrophic fishponds – impact of
607 zooplankton structure. *Aquacult. Int.*, 15, 201-210, <https://doi.org/10.1007/s10499-007-9085-2>, 2007.

608 Potužák, J., Duras, J., and Drozd, B.: Mass balance of fishponds: are they sources or sinks of phosphorus?
609 *Aquacult. Int.*, 24, 1725-1745, <https://doi.org/10.1007/s10499-016-0071-4>, 2016.

610 Prairie, Y.T. and del Giorgio, P.A.: A new pathway of freshwater methane emissions and the putative importance
611 of microbubbles. *Inland Waters*, 3, 311-320, <https://doi.org/10.5268/IW-3.3.542>, 2013.

612 Procházková, L.: Bestimmung der Nitrate im Wasser. *Zeitschrift für Analytische Chemie*, 167, 254-260, 1959.

613 Rasilo, T., Prairie, Y.T., and del Giorgio, P.A.: Large-scale patterns in summer diffusive CH₄ fluxes across boreal
614 lakes, and contribution to diffusive C emissions. *Glob. Change Biol.*, 21, 1124-1139,
615 <https://doi.org/10.1111/gcb.12741>, 2015.

616 R Core Team: A language and environment for statistical computing. R Foundation for Statistical Computing,
617 Vienna, Austria <https://www.R-project.org/>, 2018.

618 Reynolds, C.S.: Ecology of phytoplankton, Cambridge University Press, Cambridge,
619 <https://doi.org/10.1017/CBO9780511542145>, 2006.

620 Rinke, K., Huber, A.M.R., Kempke, S., Eder, M., Wolf, T., Probst, W.N., and Rothhaupt, K.: Lake-wide
621 distributions of temperature, phytoplankton, zooplankton, and fish in the pelagic zone of a large lake. *Limnol.*
622 *Oceanogr.*, 54, 1306-1322, <https://doi.org/10.4319/lo.2009.54.4.1306>, 2009.

623 Rutegwa, M., Potužák, J., Hejzlar, J., and Drozd, B.: Carbon metabolism and nutrient balance in a hypereutrophic
624 semi-intensive fishpond. *Knowl.Manag. Aquat. Ecosyst.*, 49, <https://doi.org/10.1051/kmae/2019043>, 2019.

625 Sanseverino, A.M., Bastviken, D., Sundh, I., Pickova, J., and Enrich-Prast, A.: Methane carbon supports aquatic
626 food webs to the fish level. *PLoS One*7, e42723, <https://doi.org/10.1371/journal.pone.0042723>, 2012.

627 Scheffer, M.: Ecology of shallow lakes. Population and Community Biology Series. Springer, 357 p.,
628 <https://doi.org/10.1007/978-1-4020-3154-0>, 2004.

629 Schilder, J., Bastviken, D., van Hardenbroek, M., Kankaala, P., Rinta, P., Stötter, T., and Heiri, O.: Spatial
630 heterogeneity and lake morphology affect diffusive greenhouse gas emission estimates of lakes. *Geophys. Res.*
631 *Let.*, 40, 5752-5756, <https://doi.org/10.1002/2013GL057669>, 2013.

632 Schmiedeskamp, M., Praetzel, L.S.E., Bastviken, D., and Knorr, K.H.: Whole-lake methane emissions from two
633 temperate shallow lakes with fluctuating water levels: Relevance of spatiotemporal patterns. *Limnol. Oceanogr.*,
634 66, 2455-2469, <https://doi.org/10.1002/lno.11764>, 2021.

635 Schubert, C.J., Diem, T., Eugster W.: Methane emissions from a small wind shielded lake determined by eddy
636 covariance, flux chambers, anchored funnels, and boundary model calculations: a comparison. *Environ. Sci.*
637 *Technol.*, 46, 4515-4522, <https://doi.org/10.1021/es203465x>, 2012

638 Stanley, E.H., Collins, S.M., Lottig, N.R., Oliver, S.K., Webster, K.E., Cheruvilil, K.S., and Soranno, P.A.: Biases
639 in lake water quality sampling and implications for macroscale research. *Limnol. Oceanogr.*, 64, 1572-1585,
640 <https://doi.org/10.1002/lno.11136>, 2019.

641 Stockwell, J.D., Doubek, J.P., Adrian, R., Anneville, O., Carey, C.C., Carvalho, L., Domis, L.N.D.S., Dur, G.,
642 Frassl, M.A., Grossart, H.-P., Ibelings, B.W., Lajeunesse, M.J., Lewandowska, A.M., Llames, M.E., Matsuzaki,
643 S.-I.S., Nodine, E.R., Nöges, P., Patil, V.P., Pomati, F., Rinke, K., Rudstam, L.G., Rusak, J.A., Salmaso, N.,
644 Seltmann, C.T., Straile, D., Thackeray, S.J., Thiery, W., Urrutia-Cordero, P., Venail, P., Verburg, P., Woolway,
645 R.I., Zohary, T., Andersen, M.R., Bhattacharya, R., Hejzlar, J., Janatian, N., Kpodonu, A.T.N.K., Williamson,
646 T.J., and Wilson, H.L.: Storm impacts on phytoplankton community dynamics in lakes. *Glob. Change Biol.*, 26,
647 2756-2784, <https://doi.org/10.1111/gcb.15033>, 2020.

648 van Bergen, T.J.H.M., Barros, N., Mendonça, R., Aben, R.C.H., Althuisen, I.H.J., Huszar, V., Lamers, L.P.M.,
649 Lüring, M., Roland, F., Kosten, S.: Seasonal and diel variation in greenhouse gas emissions from an urban pond
650 and its major drivers. *Limnol. Oceanogr.*, 64, 2129-2139, <https://doi.org/10.1002/lno.11173>, 2019.

651 Varadharajan, Ch. and Hemond, H.F.: Time-series analysis of high-resolution ebullition fluxes from a stratified,
652 freshwater lake. *J. Geophys. Res.*, 117, G02004, <https://doi.org/10.1029/2011JG001866>, 2012.

653 Wanninkhof, R.: Relationship between wind speed and gas exchange over the ocean revisited. *Limnol. Oceanogr.*
654 *Methods*, 12, 351-362, <https://doi.org/10.4319/lom.2014.12.351>, 2014.

655 Wiesenburg, D.A. and Guinasso N.L.: Equilibrium solubilities of methane, carbon monoxide, and hydrogen in
656 water and sea water. *J. Chem. Eng. Data*, 24, 356-360, <https://doi.org/10.1021/je60083a006>, 1979.

657 Wik, M., Varner, R.K., Anthony, K.W., MacIntyre, S., and Bastviken, D.: Climate-sensitive northern lakes and
658 ponds are critical components of methane release. *Nat. Geosci.*, 9, 99-105, <https://doi.org/10.1038/ngeo2578>,
659 2016.

660 Xiao, Q., Zhang, M., Hu, Z., Gao, Y., Hu, Ch., Liu, Ch., Liu, S., Zhang, Z., Zhao, J., Xiao, W., and Lee, X.: Spatial
661 variations of methane emission in a large shallow eutrophic lake in subtropical climate. *J. Geophys. Res.*
662 *Biogeosci.*, 122, <https://doi.org/10.1002/2017JG003805>, 2017.

663 Yamamoto, S., Alcauskas, J.B., and Crozier, T.E. Solubility of methane in distilled water and seawater. *J. Chem.*
664 *Eng. Data*, 21, 78-80, <https://doi.org/10.1021/je60068a029>, 1976.

665 Yan, X., Xu, X., Ji, M., Zhang, Z., Wang, M., Wu, S., Wang, G., Zhang, Ch., and Liu, H.: Cyanobacteria blooms:
666 A neglected facilitator of CH₄ production in eutrophic lakes. *Sci. Total Environ.*, 651, 466-474,
667 <https://doi.org/10.1016/j.scitotenv.2018.09.197>, 2019.

668 Yang, P., Zhang, Y., Yang, H., Zhang, Y., Xu, J., Tan, L., Tong, C., and Lai, D.Y.: Large fine-scale spatiotemporal
669 variations of CH₄ diffusive fluxes from shrimp aquaculture ponds affected by organic matter supply and aeration
670 in Southeast China. *J. Geophys. Res. Biogeosci.*, 124, 1290-1307, <https://doi.org/10.1029/2019JG005025>, 2019.

671 Yang, P., Zhang, Y., Yang, H., Guo, Q., Lai, D.Y.F., Zhao, G., Li, L., and Tong, C.: Ebullition was a major
672 pathway of methane emissions from the aquaculture ponds in Southeast China. *Water Res.*, 184, 116176,
673 <https://doi.org/10.1016/j.watres.2020.116176>, 2020.

674 Yuan, J., Xiang, J., Liu, D.Y., Kang, H., He, T.H., Kim, S., Lin, Y.X., Freeman, C., and Ding, W.X.: Rapid growth
675 in greenhouse gas emissions from the adoption of industrial-scale aquaculture. *Nat. Clim. Chang.*, 9, 318-322,
676 <https://doi.org/10.1038/s41558-019-0425-9>, 2019.

677 Yuan, J., Liu, D., Xiang, J., He, T., Kang, H., and Ding, W.: Methane and nitrous oxide have separated production
678 zones and distinct emission pathways in freshwater aquaculture ponds. *Water Research*, 190, 116739,
679 <https://doi.org/10.1016/j.watres.2020.116739>, 2021.

680 Zar, J.H.: *Biostatistical analysis*. Prentice Hall, Inc., Englewood Cliffs, New York, 663 p., 1984.

681 Zhang, L., Liao, Q., Gao, R., Luo, R., Liu, Ch., Zhong, J., and Wang, Z.: Spatial variations in diffusive methane
682 fluxes and the role of eutrophication in a subtropical shallow lake. *Sci. Total Environ.*, 759, 143495,
683 <https://doi.org/10.1016/j.scitotenv.2020.143495>, 2021.

684 Zhao, J., Zhang, M., Xiao, W., Jia, L., Zhang, X., Wang, J., Zhang, Z., Xie, Y., Yini Pu, Liu, S., Feng, Z., Lee X.:
685 Large methane emission from freshwater aquaculture ponds revealed by long-term eddy covariance observation.
686 *Agric. For. Meteorol.*, 308-309, 108600, <https://doi.org/10.1016/j.agrformet.2021.108600>, 2021.

687 Zhou, Y.Q., Zhou, L., Zhang, Y.L., de Souza, J.G., Podgorski, D.C., Spencer, R.G.M., Jeppesen, E., and Davidson,
688 T.A.: Autochthonous dissolved organic matter potentially fuels methane ebullition from experimental lakes. *Water*
689 *Res.*, 166, 115048, <https://doi.org/10.1016/j.watres.2019.115048>, 2019.

690 Zuur, A.F., Ieno, E.N., Walker, N.J., Saveliev, A.A., and Smith, G.M.: *Mixed effects models and extensions in*
691 *ecology with R*. Springer, New York, USA, 574 p, <https://doi.org/10.1007/978-0-387-87458-6>, 2009.

692

